Achromatic wavefront forming with space-variant polarizers: Application to phase singularities and light focusing

José A. Ferrari,[1] Wolfgang Dultz,[2] Heidrun Schmitzer,[3] and Erna Frins[1]
[1]*Facultad de Ingeniería, Instituto de Física, J. Herrera y Reissig 565, 11300 Montevideo, Uruguay*
[2]*Physikalisches Institut, Johann Wolfgang Goethe-Universität, PF 111932, D-60054 Frankfurt am Main, Germany*
[3]*Department of Physics, Xavier University 3800 Victory Parkway, Cincinnati, Ohio 45207, USA*
(Received 7 August 2007; published 13 November 2007)

We investigate the polarization-to-phase conversion of space-variant polarized light waves. Our analysis can be considered as an extension of Pancharatnam's phase to the case of space-variant polarization. In two particular cases—azimuthally and radially variant polarization—we found striking consequences. Using an azimuthally variant polarizer combined with a circular analyzer, it is possible to induce spin-to-orbital angular momentum exchange and to generate optical vortices of arbitrary charge. Radially variant polarizers with linear or quadratic radial dependence of the transmission direction generate nondiffracting beams or focus light, respectively. Our results are potentially relevant for the design of achromatic wavefront forming (and correcting) elements based strictly on space-variant polarization optics.

DOI: 10.1103/PhysRevA.76.053815 PACS number(s): 42.25.−p, 42.79.−e, 42.25.Ja

I. INTRODUCTION

Space-variant polarizers (i.e., inhomogeneous polarizers) are striking optical elements with interesting properties and applications. In particular, radial (and azimuthal) polarizers have recently attracted increased interest. For example, radially polarized light fields have been used to increase focus sharpness [1–4] and to achieve superresolution [5]. Also, other applications like particle trapping [6] and generation of optical vortices [7–9] have been reported. Radially polarized light fields have been achieved using space-variant birefringent elements [1,5,7,9–12], subwavelength gratings [13], and conical prisms [14–16].

In spite of the large amount of work devoted to this topic, a general analysis of space-variant polarized light waves is lacking. The purpose of this work is to investigate the spatial phase modulation generated by space-variant polarizers. In particular, we will discuss phase effects induced by azimuthally and radially variant polarizers. We will demonstrate theoretically and experimentally that optical vortices of arbitrary topological charge can be generated using azimuthally variant polarizers, while radially variant polarizers can be used to generate nondiffracting Bessel beams and to achieve sharp beam focusing.

To the best of our knowledge, in the literature there are no references to spatial phase effects associated with general space-variant polarized waves [17].

In Secs. II and III we describe the theory of the polarization-to-phase conversion and in Sec. IV we present validation experiments.

II. POLARIZATION-TO-PHASE CONVERSION

Let us consider a monochromatic plane wave traveling along the z axis characterized by the electric field $\vec{E}_{\mathrm{in}}$, which is incident on a polarizer lying in the xy plane (see Fig. 1). If the polarizer has its transmission direction along the unit vector $\hat{p}$ forming an angle θ with respect to the x axis, in a vector-column representation one has $\hat{p}=\binom{\cos\theta}{\sin\theta}$. The Jones matrix of the polarizer can be written as the dyadic product $\hat{p}\hat{p}$.

Now, assume that after the polarizer there is a $\lambda/4$ waveplate (with its fast axis along the x axis) and an analyzer with its transmission direction along the unit vector $\hat{p}_{\pm 45}$ at $\pm 45°$ with respect to the waveplate fast axis, as shown in Fig. 1. The output field $\vec{E}_{\mathrm{out}}$ will be given by

$$\vec{E}_{\mathrm{out}} = \hat{p}_{\pm 45}\hat{p}_{\pm 45}\cdot W\cdot\hat{p}\hat{p}\cdot\vec{E}_{\mathrm{in}} = \hat{p}_{\pm 45}(\hat{p}_{\pm 45}\cdot W\cdot\hat{p})(\hat{p}\cdot\vec{E}_{\mathrm{in}}), \tag{1}$$

where $W=\begin{pmatrix}1 & 0\\ 0 & i\end{pmatrix}$ is the Jones matrix of the $\lambda/4$ waveplate.

It is easily verified that $\hat{p}_{\pm 45}\cdot W\cdot\hat{p}=(1/\sqrt{2})\exp(\pm i\theta)$, so that the expression (1) can be rewritten in the form

$$\vec{E}_{\mathrm{out}} = (1/\sqrt{2})(\hat{p}\cdot\vec{E}_{\mathrm{in}})\exp(\pm i\theta)\hat{p}_{\pm 45}. \tag{2}$$

Thus, the combination "arbitrary polarizer"–"$\lambda/4$ waveplate"–"analyzer at $\pm 45°$" provides a polarization-to-phase conversion, i.e., a polarization angle θ is converted into a phase factor $\exp(\pm i\theta)$.

The appearance of the phase factor $\exp(\pm i\theta)$ can be interpreted as a consequence of the fact that a linearly polarized wave can be decomposed into a linear combination of phase-shifted right and left circularly polarized waves, and that the combination $\lambda/4$ waveplate–analyzer at $\pm 45°$ is a circular

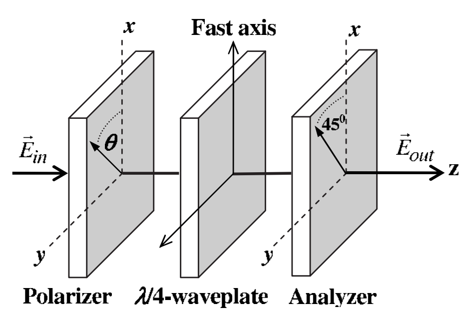

FIG. 1. Polarization-to-phase conversion.

 ©2007 The American Physical Society

analyzer. In the next sections we will demonstrate that this apparently trivial polarization-to-phase conversion has important consequences when applied to *space-variant polarizers*.

Notice that $\hat{p}_{\pm 45}\cdot W\cdot\hat{p}=\hat{p}\cdot W\cdot\hat{p}_{\pm 45}$, and thus the combination "polarizer at ±45°" – "λ/4 waveplate"–"arbitrary polarizer" provides also a phase conversion. This last combination of polarizers and λ/4 waveplate is often used in interferometric devices with geometric (Pancharatnam) phase control (see, e.g., [18,19]).

Finally, in Eq. (2) the factor $\hat{p}\cdot\vec{E}_{\text{in}}$ can eventually provide an additional phase modulation. For example, when the incident wave is circularly polarized with amplitude E_0, we will have $\vec{E}_{\text{in}}=E_0\binom{1}{\sigma i}$, where $\sigma=\pm 1$ is the helicity of the wave. In this case $\hat{p}\cdot\vec{E}_{\text{in}}=E_0\exp(i\sigma\theta)$, and thus, substituting this last expression in (2), we obtain

$$\vec{E}_{\text{out}}=(E_0/\sqrt{2})\exp[i(\sigma\pm 1)\theta]\hat{p}_{\pm 45}. \tag{3}$$

III. SPACE-VARIANT POLARIZERS

Space-variant polarizers are inhomogeneous polarizers in which the angle θ (of the transmission direction with respect to the x axis) changes point to point on the polarizer surface; that is, $\theta=\theta(x,y)$. From (3), we have

$$\vec{E}_{\text{out}}(x,y)=(E_0/\sqrt{2})\exp[i(\sigma\pm 1)\theta(x,y)]\hat{p}_{\pm 45}. \tag{4}$$

Thus, the output field has two phase modulations with different origins; one of them is due to the interaction of the incident circularly polarized wave with the space-variant polarizer, and the other contribution is due to the interaction of the (space-variant) polarized wave with a circular analyzer. In the following, we will discus particular cases of space-variant polarizers.

A. Azimuthally variant polarizers

Let (r,φ) be the radial and angular coordinates, respectively, of an arbitrary point (x,y) on the space-variant polarizer. Azimuthally variant polarizers are those in which the transmission direction depends only on the polar angle φ. In the literature, a particular case of azimuthally variant polarizer in which the transmission direction is characterized by $\theta(\varphi)=\varphi$ is called a *radial polarizer*, while a polarizer with $\theta(\varphi)=\varphi+\pi/2$ is often called an *azimuthal polarizer*, as shown in Figs. 2(a) and 2(b). Thus, a radial polarizer should not be confused with a radially variant polarizer, which will be studied in Sec. III B.

In fact, there are many types of azimuthally variant polarizers that cannot be strictly classified as azimuthal or radial polarizers. A simple example of this situation is the case when $\theta(\varphi)=\varphi+a_0$ with a_0=const $(\neq 0,\pi/2,\pi,\ldots)$. Although a_0 destroys the symmetry of the polarizer, the resultant phase modulation is essentially the same as for radial and azimuthal polarizers, because in general a constant phase factor $\exp[i(\sigma\pm 1)a_0]$ does not have measurable consequences.

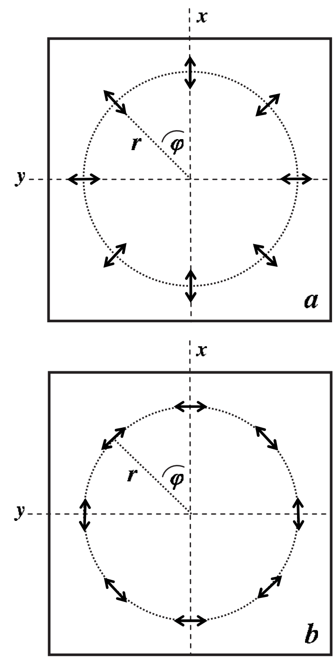

FIG. 2. (a) Radial polarizer; (b) azimuthal polarizer.

Another example that cannot be strictly classified as a radial or an azimuthal polarizer is the case when $\theta(\varphi)=n\varphi$ with n integer (and $n\neq 0,1$). Figures 3(a) and 3(b) show the situation for $n=-1$ and 2, respectively.

Now, consider the particular case in which a circularly polarized plane wave $(\vec{E}_{\text{in}})$ is incident on an azimuthally variant polarizer with polarization direction characterized by the angular dependence $\theta(\varphi)=n\varphi+a_0$, where n is an integer and a_0 is constant. From (4) we have

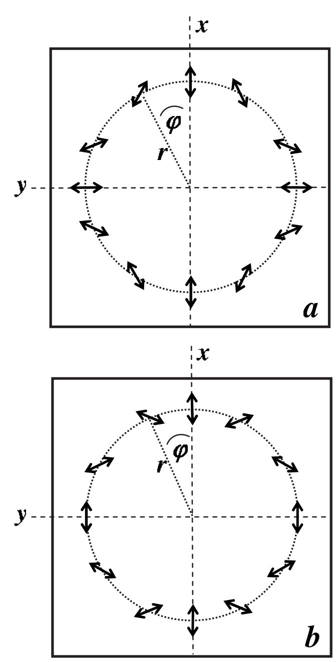

FIG. 3. Azimuthally variant polarizers with $\theta(\varphi)=n\varphi$. $n=$ (a) -1; (b) 2.

$$\vec{E}_{\text{out}}(\varphi) = E_0' \exp[i(\sigma \pm 1)n\varphi]\hat{p}_{\pm 45}, \tag{5}$$

where $E_0' = (E_0/\sqrt{2})\exp[i(\sigma \pm 1)a_0]$.

Thus, at the output of the system we will have a helical beam with azimuthal number $l=(\sigma\pm 1)n$. In other words, with the combination of an azimuthally variant polarizer, a $\lambda/4$ waveplate and an analyzer at $\pm 45°$, it is possible to generate an optical vortex with arbitrary topological charge $l=(\sigma\pm 1)n$. The resultant topological charge will depend on the helicity of the incident beam (σ) and on the orientation of the analyzer $\hat{p}_{\pm 45}$. Both contributions to the phase can be reinterpreted in terms of spin-to-orbital angular momentum exchanges between light and matter. (For a discussion of the spin-to-orbital angular momentum exchange in inhomogeneous anisotropic media, see, e.g., Marrucci *et al.* [9].)

These independent contributions to the phase can reinforce or cancel each other. For example, if the incident wave is circularly polarized with $\sigma=1$ and the analyzer is at $-45°$ with respect to the x axis, the resultant topological charge will be zero independently of the azimuthally variant polarizer, and then we will recover a plane wave without phase singularity along the propagation axis. On the other hand, when the analyzer is at $+45°$ with respect to the x axis, we will obtain an optical vortex with double topological charge, $l=2n$. In fact, the circular polarization of the incident wave is not an essential requirement for the existence of phase singularities, as clearly shown in (2). For example, even if we have an incident linearly polarized wave, we will obtain at the output an optical vortex (with space-variant amplitude $\vec{E}_{\text{in}}\cdot\hat{p}$). Its topological charge will be $l=\pm n$ depending on the $\pm 45°$ analyzer orientation with respect to the x axis.

The striking issue to be noted is that the existence (or not) of the phase singularity depends on the orientation of an analyzer, which does not possess singularity at any point on its surface. Equivalently, instead of mechanically changing the analyzer orientation, it is possible to interchange the fast and slow axes of the $\lambda/4$ waveplate using an electro-optical device, e.g., a Pockels or Kerr cell. In this way the optical vortex could be electrically switched.

B. Radially variant polarizers

A radially variant polarizer is a special case of a space-variant one in which $\theta=\theta(r)$, i.e., there is no angular dependence, as in the example shown in Fig. 4. To the best of our knowledge, this kind of polarizer has not been studied in the literature.

Let us now consider a circularly polarized monochromatic plane wave ($\vec{E}_{\text{in}}$) incident on a radially variant polarizer with polarization direction characterized by the angle $\theta(r)$. From (4), we have

$$\vec{E}_{\text{out}}(r) = (E_0/\sqrt{2})\exp[i(\sigma \pm 1)\theta(r)]\hat{p}_{\pm 45}. \tag{6}$$

Hence, the output field has a radial phase modulation which can be used for light focusing. For example, let us consider the particular case when $\theta(r)=\alpha r+b_0$ with α and b_0 being constants. From (6) we obtain

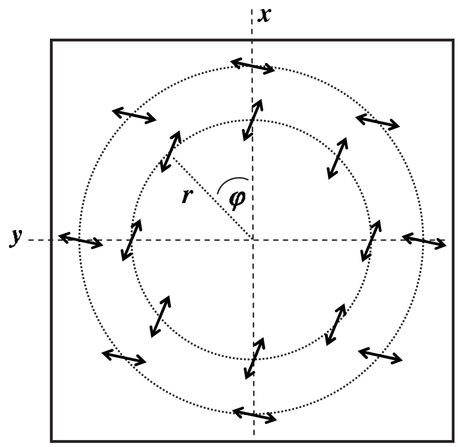

FIG. 4. Example of radially variant polarizer.

$$\vec{E}_{\text{out}}(r) = E_0' \exp[i(\sigma \pm 1)\alpha r]\hat{p}_{\pm 45}, \tag{7}$$

where $E_0' = (E_0/\sqrt{2})\exp[i(\sigma \pm 1)b_0]$.

Thus, the outgoing wave has an axiconlike phase factor $\exp[i(\sigma\pm 1)\alpha r]$, where $(\sigma\pm 1)\alpha$ is the component of the wave vector in the radial direction (k_r). A negative phase $(\sigma\pm 1)\alpha r<0$ means a positive axicon, which will produce a J_0 Bessel beam around the propagation axis, i.e., a nondiffracting beam with nonvanishing intensity on the axis [20].

Now, let us consider the case when $\theta(r)=\beta r^2+b_0$, where β and b_0 are constants. From (6) we obtain

$$\vec{E}_{\text{out}}(r) = E_0' \exp[i(\sigma \pm 1)\beta r^2]\hat{p}_{\pm 45}. \tag{8}$$

Hence we conclude that the combination of a polarizer with quadratic radial dependence, a $\lambda/4$ waveplate, and an analyzer at $\pm 45°$ works as a lens with focal length f given by

$$f = -\pi/(\sigma \pm 1)\beta\lambda. \tag{9}$$

When $(\sigma\pm 1)\beta<0$, the outgoing wave ($\vec{E}_{\text{out}}$) represents a sharply focused light beam. Thus, the value of f will depend on the helicity (σ) of the incident wave, on the factor β which is characteristic of the radially variant polarizer, and on the $\pm 45°$ orientation of the analyzer. In other words, the device works like a switchable lens. For example, if the incident wave is circularly polarized with $\sigma=1$ and the analyzer is at $-45°$ with respect to the x axis, the lens effect will be "off" (i.e., "infinite" focal length). On the other hand, when the analyzer is at $+45°$ with respect to the waveplate fast axis, one obtains a lens of finite focal length $f=-\pi/2\beta\lambda$, which will be positive or negative depending on the sign of β. Equivalently, instead of mechanically changing the $\pm 45°$ analyzer orientation, it is also possible to interchange the fast and slow axes of the $\lambda/4$ waveplate using an electro-optical device, e.g., a Pockels or Kerr cell.

IV. EXPERIMENTAL RESULTS

A. Setup

We have performed some experiments to illustrate the generation of a desired phase modulation starting from the

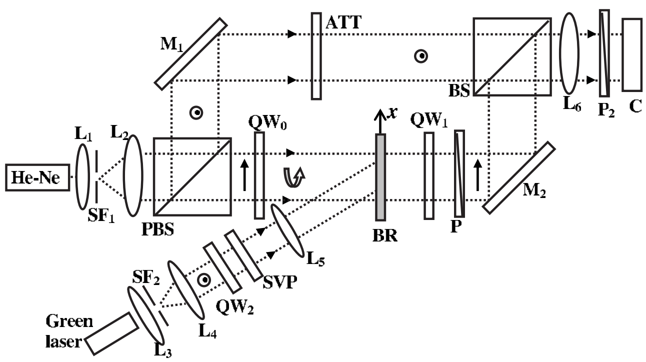

FIG. 5. Experimental setup.

corresponding space-variant polarizer. To do this, it is necessary to use high-optical-quality polarizers without phase noise.

The complete setup is shown in Fig. 5. It consists in a Mach-Zehnder interferometer with a polarized He-Ne laser ($\lambda = 633$ nm, 1 mW) as light source, and an *external system* with a polarized green laser ($\lambda = 532$ nm, 10 mW) as light source. The Mach-Zehnder interferometer is utilized to verify the existence of the desired phase distribution, while the external system induces a space-variant polarizer of high optical quality on a *Bacteriorhodopsin* (BR) film (variant DN96, OD 4, provided by MIB GmbH) [21,22].

In one of the interferometer arms we have inserted the polarization-to-phase converter (formed by the BR film, the $\lambda/4$ waveplate QW_1, and the analyzer P), which has the function of converting the space-variant polarization into a space-variant phase profile.

Next we will describe the details of the setup shown in Fig. 5. The expanded He-Ne laser beam is split with the help of a polarizing beam splitter (PBS) into two linearly polarized beams. To describe the setup it is convenient to choose the x axis lying in the plane of Fig. 5. Then, the field amplitude of the light wave incident on the $\lambda/4$ waveplate QW_0 can be written as

$$E_{\text{He-Ne}} = E_0 \begin{pmatrix} 1 \\ 0 \end{pmatrix} \tag{10}$$

with E_0 constant. The waveplate QW_0 has its fast axis at 45° with respect to the x direction; thus it will be characterized by the matrix

$$M = \begin{pmatrix} 1 & i \\ i & 1 \end{pmatrix}, \tag{11}$$

where we have omitted some unimportant factors. (The waveplate is rotated 45° with respect to the orientation chosen for doing the calculations in Secs. II and III.)

Thus, after QW_0 we will have a circularly polarized wave

$$E_{\text{QW}} = E_0 \begin{pmatrix} 1 \\ i \end{pmatrix}, \tag{12}$$

which "reads" the polarization pattern induced on the BR by the green light.

The $\lambda/4$ waveplate QW_1 has its fast axis parallel to that of QW_0, so that it will also be characterized by the matrix M.

When the BR is not illuminated by green light, there is no polarization information saved on the BR. Hence, the state of polarization of the incident (reading) He-Ne beam will not change. In this case, after QW_1 we have a polarization state orthogonal to that before QW_0. After QW_1 there is an analyzer (P) with its transmission direction at +45° with respect to the QW_1 fast axis, i.e., along the x axis,

$$\hat{p}_{+45} = \begin{pmatrix} 1 \\ 0 \end{pmatrix}, \tag{13}$$

which is blocking the direct He-Ne beam.

Due to the light-induced dichroism of the BR, the incident (writing) polarized electric field $\vec{E}_{\text{green}}(x,y)$ will induce a polarization mask on the BR film when illuminated with green light [21,22]. Its transmission matrix is given by

$$M_{\text{BR}} = (1-\gamma)I + \gamma\hat{p}\hat{p}, \tag{14}$$

where I is the unit matrix, and $\hat{p} = \begin{pmatrix} \cos\theta(x,y) \\ \sin\theta(x,y) \end{pmatrix}$ is the polarization direction of the incident (writing) wave $\vec{E}_{\text{green}}(x,y)$. $\theta(x,y)$ is the angle of $\hat{p}$ with respect to the x axis, and γ (<1) is an efficiency factor that depends on the BR type utilized in the experiments, the green-laser intensity, the room temperature, etc. In our case γ is of the order of 0.04.

The first term on the right side of (14) means that a large fraction of the incident (red) light passes through the BR without changes. This spurious light will be blocked by the analyzer at +45°, as discussed above.

The spatial polarization distribution $\theta(x,y)$ on the BR was generated using space-variant polarizers (SVPs) (Frank Woolley & Co., Reading PA), with the same polarization distribution. The SVP was illuminated with a circularly polarized wave generated by a $\lambda/4$ waveplate QW_2 (for 532 nm) with its fast axis at 45° with respect to the incident polarized wave. The "image" of the SVP that is projected (using the lens L_5) on the BR is not an amplitude-modulated image, but an image of the polarization distribution [23].

The available space-variant polarizers cannot be used directly in the interferometric setup to generate the desired phase distributions, because they show a high level of phase noise. In contrast to this, the polarization distribution induced on the BR film is of high optical quality, since the BR is not sensitive to the phase noise of the incident (writing) wave $\vec{E}_{\text{green}}(x,y)$.

In our experimental setup, the (x,y) plane of the BR is slightly tilted with respect to the plane of the SVP, which could generate a small angular distortion of the polarization distribution (i.e., a distorted image of the SVP) on the BR. This distortion is not relevant for our purposes. However, if we would like to have a distortion-free image of the SVP, we have to use the fact that the decay time of the BR type used in our experiments is of the order of 30 s or more (depending on the room temperature). Thus, the polarization pattern can be written on the BR film with its plane perpendicular to the

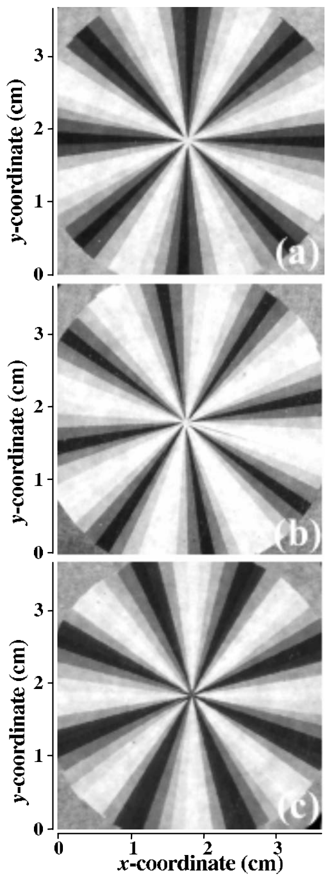

FIG. 6. Woolley's polarizer with $n=4$ viewed through a linear polarizer, for three different polarization directions in steps of $\pi/4$ (rad). (a)–(c) show three photographs with eight dark brushes, with a rotation of $\pi/16$ (rad) between consecutive images.

propagation direction of the green beam. Then, we would have up to 30 s to tilt the BR plane, and to put it perpendicular to the propagation direction of the (reading) He-Ne beam, as shown in the figure.

The combination "space-variant polarizer"–"$\lambda/4$ waveplate"–"analyzer at +45°" is placed in one of the interferometer arms, while in the other interferometer arm there is an attenuator (ATT). Both waves are recombined with a beamsplitter (BS), and finally they are brought to interfere with the help of a polarizer (P_2), which can be rotated to compensate the residual intensity differences of the two waves and achieve a high contrast interferogram. Finally, a lens (L_2) images the plane of the BR on a charge-coupled device camera (C). In the setup, $M_{1,2}$ are mirrors, $SF_{1,2}$ are spatial filters, and L_{1-4} are lenses to expand the laser beams.

B. Experiments

First we performed experiments to generate optical vortices using an azimuthally variant polarizer with linear angular dependence, $\theta(\varphi)=n\varphi$, with $n=4$ [see expression (5)]. Figures 6(a)–6(c) show this element viewed through a linearly polarizer (i.e., illuminated with linearly polarized light) for three different polarization directions in steps of $\pi/4$ (rad).

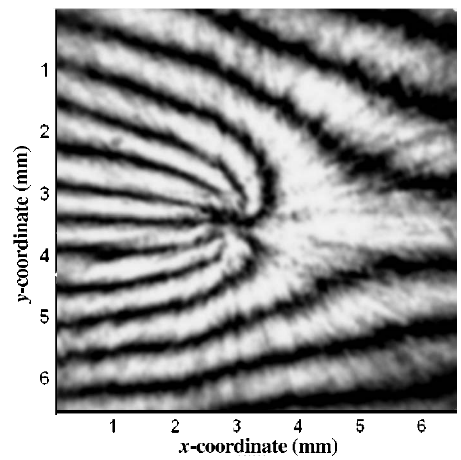

FIG. 7. Typical forklike interferogram due to an optical vortex with topological charge 8.

When $\hat{p}=\binom{\cos(4\varphi)}{\sin(4\varphi)}$ and $\vec{E}_{\text{in}}=E_0\binom{\cos(\varepsilon\pi/4)}{\sin(\varepsilon\pi/4)}$ with $\varepsilon=(0,1,2)$, the intensity pattern will be $I(\varphi)=|\hat{p}\cdot\vec{E}_{\text{in}}|^2=E_0^2\cos^2(4\varphi-\varepsilon\pi/4)=(E_0^2/2)[1+\cos(8\varphi-\varepsilon\pi/2)]$. Then the dark regions will be centered around the angular positions $\varphi_m=m\pi/8+\varepsilon\pi/16$, with m an odd integer. Thus, there are eight values of φ_m in the interval $[0,2\pi]$. Figures 6(a)–6(c) show three images with eight dark "brushes," with a rotation of $\pi/16$ (rad) between consecutive images.

With the exception of $n=1$, in all azimuthally variant polarizers manufactured by Frank Woolley and Co. the polarization changes in a discontinuous way. This does not really disturb our experiments, because the important quantity is the topological charge defined as $[(\sigma\pm1)/2\pi]\oint\vec{\nabla}\theta\cdot d\vec{s}$ (where $d\vec{s}$ is a line element on a curve enclosing the origin of coordinates), which remains invariant independently of the discontinuous polarization changes.

Figure 7 shows the interferogram produced by interference of the wavefront due to the space-variant polarizer and a slightly tilted plane reference wave. This figure shows clearly the typical forklike interferogram due to an optical vortex with topological charge 8, as theoretically predicted for $\sigma=1$ and the analyzer at +45°.

In our second experiment we used a radially variant polarizer with linear radial dependence, $\theta(r)=\alpha r$, with $\alpha\approx-2.5$ rad/mm [see expression (7)]. (This value of α is the value obtained directly on the BR film, not on the SVP.) Figures 8(a)–8(c) show this element viewed through a linear polarizer, for three different polarization directions in steps of $\pi/4$ (rad). The azimuthal rings come from the discontinuous polarization rings of the element.

Figure 9 shows the interferogram produced by interference of the wavefront due to the space-variant polarizer and a slightly tilted reference wave. On a central strip of the image, it is possible to consider that the interferogram possesses an approximately linear spatial carrier. We can apply to this central strip a method similar to that developed by

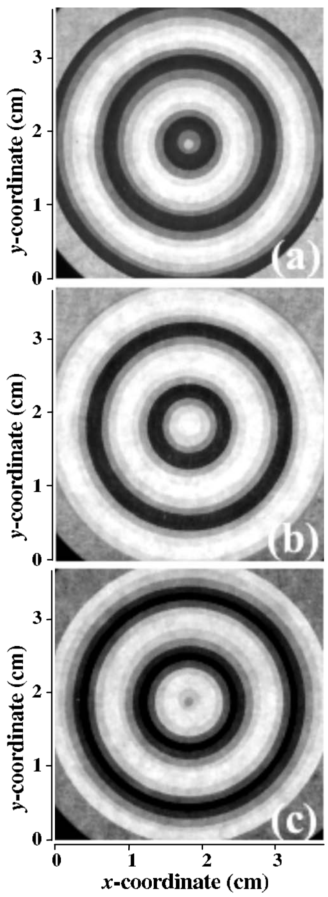

FIG. 8. Radially variant polarizer viewed through a linear polarizer, for three different polarization directions in steps of $\pi/4$ (rad).

the authors [24] for phase retrieval in interferograms with linear spatial carrier. Figure 10 shows the retrieved phase profile; the figure shows clearly an approximately linear phase profile characteristic of an axiconlike element.

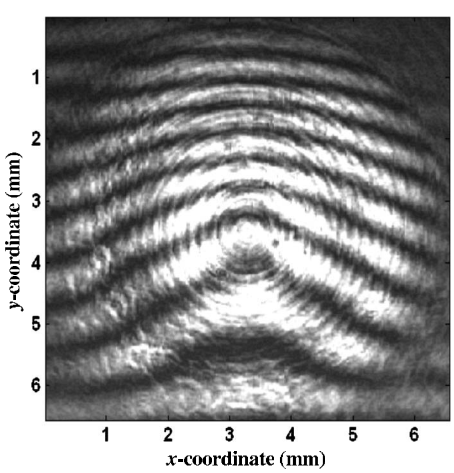

FIG. 9. Interferogram produced by interference of a wave with the phase modulation due to a polarizer with linear radial dependence and a slightly tilted wave.

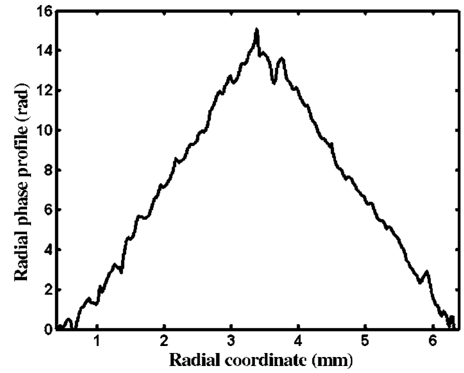

FIG. 10. Retrieved linear phase profile characteristic of axiconlike elements.

V. DISCUSSION AND CONCLUSIONS

We have demonstrated theoretically and experimentally that it is possible to generate a desired wavefront using space-variant polarizers. Some of these ideas were already (in a latent way) in the literature about the so-called topological (Pancharatnam) phase, which we have extended to include the case of space-variant polarizers. (There is a series of papers [25] devoted to wavefront generation with Pancharatnam's phase, which is achieved by the use of computer-generated subwavelength gratings.)

We have shown that the resultant spatial phase modulation $(\sigma\pm1)\theta(r,\varphi)$ has two different origins; the interaction of the incident (circular polarized) wave with the space-variant polarizer, and the interaction of the space-variant polarized wave with the circular analyzer. These independent contributions can reinforce or cancel each other.

We have performed some illustrative experiments with azimuthally and radially variant polarizers to demonstrate the generation of different phase profiles from the corresponding spatial polarization distributions. Starting with an azimuthally variant polarizer with $n=4$, we have shown that it is possible to generate an optical vortex with topological charge 8, as predicted by the theory. Also, starting with a polarizer with linear radial dependence we have generated an axiconlike phase profile.

The main problem in generating the desired phase profiles was the difficulty in finding commercially available polarizers with the required spatial distribution and the necessary optical quality. We overcame this difficulty by using the polarmotion elements of Frank Woolley, which have the desired polarization pattern, but a noisy optical thickness [26], and inducing only their dichroism onto a high-quality *Bacteriorhodopsin* film. The drawback of using BR is that, because of the its low polarizing efficiency, most of the spurious (red) light passing through BR has to be blocked with the help of an analyzer at +45°. For this reason, when the helicity is $\sigma=1$, we cannot perform experiments with the analyzer at −45° (or, equivalently, when the helicity is $\sigma=-1$, we cannot perform an experiment with the analyzer at +45°).

Finally, it is important to notice that, with the hypothesis that the waveplate could be made achromatic, the generated phase profiles will also be achromatic, because polarization is essentially a wavelength independent phenomenon. (Indeed, the polarization efficiency of a regular polarizer is wavelength dependent. However, this is not an essential characteristic of the phenomenon; it is a characteristic of the material used to make the polarizer.) Compared to direct phase modulation methods, in which usually the refractive index (or the optical path) of a phase mask is changed, this achromatic behavior is an important difference.

ACKNOWLEDGMENT

J.A.F. and E.F. acknowledge the financial support of the Comisión Sectorial de Investigación Científica (CSIC) of the Universidad de la República, Uruguay.

[1] R. Dorn, S. Quabis, and G. Leuchs, Phys. Rev. Lett. **91**, 233901 (2003).
[2] D. W. Diehl, R. W. Schoonover, and T. D. Visser, Opt. Express **14**, 3030 (2006).
[3] Y. Kozawa and S. Sato, Opt. Lett. **31**, 820 (2006).
[4] N. Bokor and N. Davidson, Opt. Lett. **29**, 1968 (2004).
[5] M. Yun, L. Liu, J. Sun, and D. Liu, J. Opt. Soc. Am. A **21**, 1869 (2004).
[6] Q. Zhang, Opt. Express **12**, 3377 (2004).
[7] F. Flossmann, U. T. Schwarz, M. Maier, and M. R. Dennis, Phys. Rev. Lett. **95**, 253901 (2005).
[8] Q. Zhan and J. R. Leger, Opt. Commun. **213**, 241 (2002).
[9] L. Marrucci, C. Manzo, and D. Paparo, Phys. Rev. Lett. **96**, 163905 (2006).
[10] P. B. Phua, W. J. Lai, Y. L. Lim, K. S. Tiaw, B. C. Lim, H. H. Teo, and M. H. Hong, Opt. Lett. **32**, 376 (2007).
[11] N. Passilly, R. de Saint Denis, K. Aït-Ameur, F. Treussart, R. Hierle, and J.-F. Roch, J. Opt. Soc. Am. A **22**, 984 (2005).
[12] Q. Zhan and J. R. Leger, Appl. Opt. **41**, 4630 (2002).
[13] Z. Bomzon, G. Biener, V. Kleiner, and E. Hasman, Opt. Lett. **27**, 285 (2002).
[14] J. Li, K. Ueda, M. Musha, A. Shirakawa, and L. Zhong, Opt. Lett. **31**, 2969 (2006).
[15] A. Shoham, R. Vander, and S. G. Lipson, Opt. Lett. **31**, 3405 (2006).
[16] J. Li, 1, K. Ueda, M. Musha, A. Shirakawa, and Z. Zhang, Opt. Lett. **32**, 1360 (2007).
[17] Zhan and Leger [8] investigated only an optical vortex of charge 1 and Marrucci *et al.* [9] studied the effect of an azimuthally variant birefringent element.
[18] E. M. Frins, W. Dultz, and J. A. Ferrari, Pure Appl. Opt.: J. Euro. Opt. Soc., Part A, **7**, 53 (1998).
[19] J. A. Ferrari, E. M. Frins, and W. Dultz, J. Lightwave Technol. **15**, 968 (1997).
[20] The sign convention used for k_r is consistent with the signs used for the phase factor of the incident plane wave traveling along the z axis, which we write as $\exp[i2\pi(z-ct)/\lambda]$, λ being the wavelength and c the light velocity of vacuum.
[21] N. Hampp, Chem. Rev. (Washington, D.C.) **100**, 1755 (2000).
[22] Y. Okada-Shudo, J.-M. Jonathan, and G. Roosen, Opt. Eng. (Bellingham) **41**, 2803 (2002).
[23] Woolley's polarizers used in our experiments come with an adhesive on one of their surfaces (which can be removed with isopropyl alcohol). The polarizer can be thought of as an "ideal polarizer" deposited on a birefringent plastic substratum. Thus, in order to preserve the polarization state of the incident wave $\vec{E}_{\text{green}}(x,y)$, it must be incident on the ideal side of the polarizer (the ideal side is the side opposite to the adhesive).
[24] J. A Ferrari and E. M. Frins, Opt. Commun. **271**, 59 (2007).
[25] Z. Bomzon, G. Biener, V. Kleiner, and E. Hasman, Opt. Lett. **27**, 1141 (2002); Z. Bomzon, V. Kleiner, and E. Hasman, *ibid.* **26**, 1141 (2001); G. Biener, A. Niv, V. Kleiner, and E. Hasman, *ibid.* **27**, 1875 (2002); A. Niv, G. Biener, V. Kleiner, and E. Hasman, *ibid.* **29**, 238 (2004).
[26] Woolley's polarizers are designed for special dichroic patterns on displays and not for interferometry.